Journal of Medicinal Chemistry

ARTICLE

pubs.acs.org/jmc

Structure-Based Design and Synthesis of 1,3-Oxazinan-2-one Inhibitors of 11β-Hydroxysteroid Dehydrogenase Type 1

Zhenrong Xu,[†] Colin M. Tice,[*,†] Wei Zhao,[†] Salvacion Cacatian,[†] Yuan-Jie Ye,[†] Suresh B. Singh,[†] Peter Lindblom,[†] Brian M. McKeever,[†] Paula M. Krosky,[†] Barbara A. Kruk,[†] Jennifer Berbaum,[†] Richard K. Harrison,[†] Judith A. Johnson,[†] Yuri Bukhtiyarov,[†] Reshma Panemangalore,[†] Boyd B. Scott,[†] Yi Zhao,[†] Joseph G. Bruno,[†] Jennifer Togias,[†] Joan Guo,[†] Rong Guo,[†] Patrick J. Carroll,[‡] Gerard M. McGeehan,[†] Linghang Zhuang,[†] Wei He,[†] and David A. Claremon[†]

[†]Vitae Pharmaceuticals, 502 West Office Center Drive, Fort Washington, Pennsylvania 19034, United States

[‡]Department of Chemistry, University of Pennsylvania, 250 South 33rd Street, Philadelphia, Pennsylvania 19104, United States

Supporting Information

ABSTRACT: Structure based design led directly to 1,3-oxazinan-2-one **9a** with an IC_{50} of 42 nM against 11β-HSD1 in vitro. Optimization of **9a** for improved in vitro enzymatic and cellular potency afforded **25f** with IC_{50} values of 0.8 nM for the enzyme and 2.5 nM in adipocytes. In addition, **25f** has 94% oral bioavailability in rat and >1000× selectivity over 11β-HSD2. In mice, **25f** was distributed to the target tissues, liver, and adipose, and in cynomolgus monkeys a 10 mg/kg oral dose reduced cortisol production by 85% following a cortisone challenge.

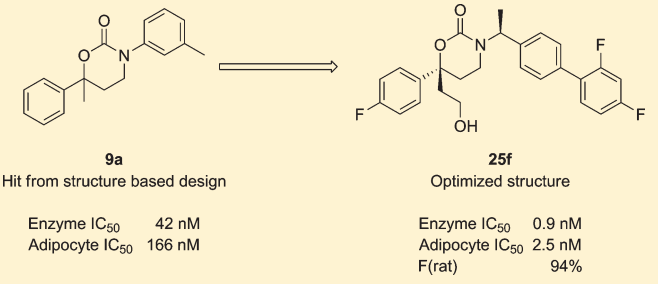

INTRODUCTION

Diabetes is an abnormal state marked by an inability to make sufficient insulin (type 1 diabetes) or by an inability to appropriately respond to insulin (type 2 diabetes). Both conditions lead to elevated concentrations of glucose in the blood. The estimated global diabetes prevalence in 2010 is 285 million and is predicted to rise to 438 million by 2030 (IDF, Diabetes Atlas).[1] When left untreated, diabetes results in serious complications including cardiovascular disease, renal failure, and retinal damage. Moreover, diabetes is often associated with comorbidities of obesity, dyslipidemia, and hypertension. This assembly of diseases is known as metabolic syndrome.[2] Current therapies include life style intervention, oral antidiabetes drugs, and injections of insulin or incretin mimetics. The need for novel, safe, and easy to administer alternatives persists because of inadequate improvement in glycemic control and/or intolerable side effects.[3] In recent years, advances in understanding the fundamental biology underlying the diseases comprising metabolic syndrome have raised possibilities for pharmacological interventions that directly impact their etiology and progression. One enzyme proposed to be critical for the development of metabolic syndrome is 11β-hydroxysteroid dehydrogenase type 1 (11β-HSD1), a member of the short chain dehydrogenase/reductase (SDR) superfamily[4,5] responsible for the local activation of inactive cortisone to the active glucocorticoid cortisol.

Plasma cortisol is primarily synthesized de novo in the zona fasciculata of the adrenal cortex in response to stimuli from the hypothalamic−pituitary−adrenal axis (HPA).[6,7] Cortisol binds to and activates the glucocorticoid receptor, resulting in increased expression of a wide range of genes involved in metabolism, immune response, bone formation, memory, and reproduction. More specifically, cortisol drives gluconeogenesis in the liver and adipogenesis in adipose tissue, which when elevated may contribute to metabolic syndrome. Circulating levels of cortisol are tightly controlled through the HPA axis, as well as by binding to corticosteroid-binding globulin and serum albumin and by inactivation to cortisone by 11β-hydroxysteroid dehydrogenase type 2 (11β-HSD2), an NAD-dependent oxidase expressed primarily in the kidney.[8]

However, tissue-specific and intracellular concentrations of cortisol vary from plasma levels primarily because of the expression and activity of 11β-HSD1 and 11β-HSD2.[9] NADPH-dependent 11β-HSD1 is primarily expressed in liver and adipose tissue, and its elevated expression in adipose tissue has been linked to obesity, insulin resistance, diabetes, and cardiovascular disease in humans.[10−14] There is considerable overlap between the symptoms of hypercortisolism (Cushing's syndrome) and those of the metabolic syndrome.[15] Transgenic mice selectively overexpressing 11β-HSD1 in adipose tissue exhibit visceral obesity, insulin resistance, and hypertension,[16,17] while 11β-HSD1 knockout mice are resistant to diet induced obesity and have increased insulin sensitivity.[18−20] Thus, a selective inhibitor of 11β-HSD1 may lower tissue-specific levels of cortisol and may

Received: May 3, 2011
Published: July 25, 2011

 © 2011 American Chemical Society

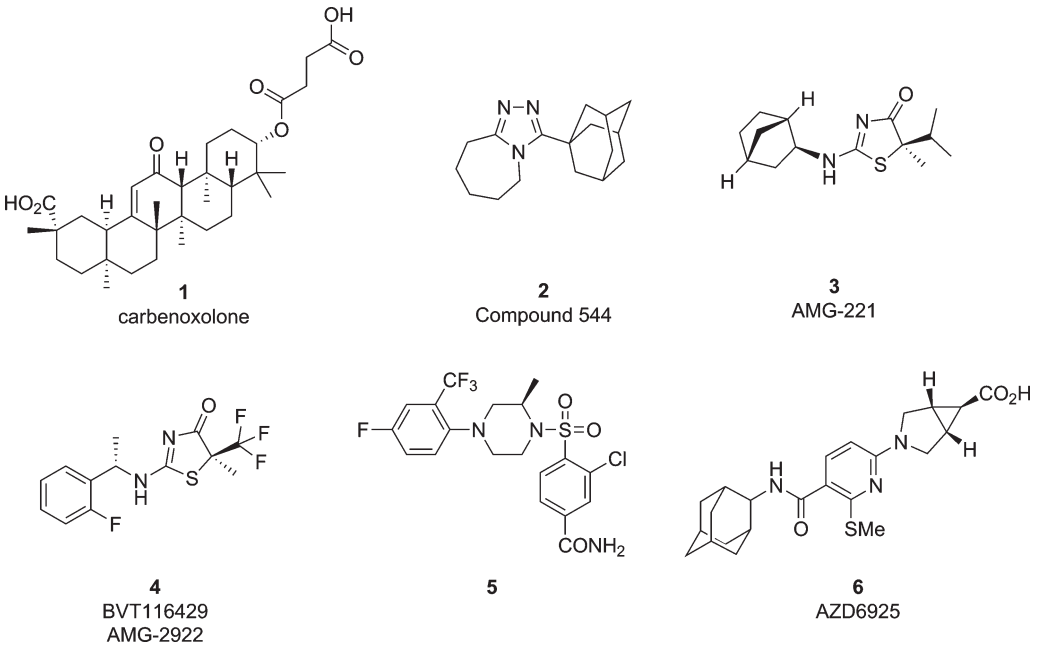

Figure 1. Literature 11β-HSD1 inhibitors.

be useful for the treatment of diabetes and other morbidities associated with metabolic syndrome.

Carbenoxolone (**1**, Figure 1), a semisynthetic derivative of the natural product 18β-glycyrrhetinic acid, is a nonselective inhibitor of 11β-HSD1 and of 11β-HSD2. Despite its lack of selectivity for 11β-HSD1, **1** has been investigated in animal and human studies where it improved insulin sensitivity.[21,22] Since 2002,[23] several classes of more selective, synthetic inhibitors of 11β-HSD1 have been reported.[24−26] Triazole **2** increased insulin sensitivity and decreased fasting glucose, cholesterol, and adipose tissue mass in mice.[27] Thiazolone **3** dosed at 25 mg/kg b.i.d. for 13 days to mice with DIO reduced fed blood glucose and plasma insulin levels.[28] Oral dosing of thiazolone **4** has been reported to increase plasma adiponectin levels and decrease fasting glucose levels in KKA$^{\gamma}$ mice.[29,30] Sulfonamide **5** has been shown to reduce fed glucose and fasted insulin in mice when incorporated into a high fat diet at 30 (mg/kg)/day.[31] The activity of these compounds in animal models further validates the potential for selective inhibitors of 11β-HSD1 in the treatment of diabetes.

Several 11β-HSD1 inhibitors are reported to have entered clinical trials, including adamantylamide **6**.[32] When added to ongoing metformin therapy in a phase 2 trial, a 200 mg dose of INCB13739 (structure not disclosed) reduced HBA1C by 0.6% and fasting plasma glucose by 24 mg/dL.[33] A 6 mg/day dose of MK-0916 (structure not disclosed) in a phase 2 trial in patients with type 2 diabetes did not improve fasting plasma glucose; however, modest improvements in HBA1C, body weight, and blood pressure were observed.[34]

DISCUSSION OF ENZYME STRUCTURE

Prior to initiation of our medicinal chemistry program, we examined the crystal structures of 11β-HSD1 that were publicly available at that time (PDB codes 1XSE, 1XU7, 1XU9, 1Y5M, 1Y5R, 2BEL). In 11β-HSD1, Ser170 and Tyr183, along with the cofactor NADPH, are key elements involved in the catalytic

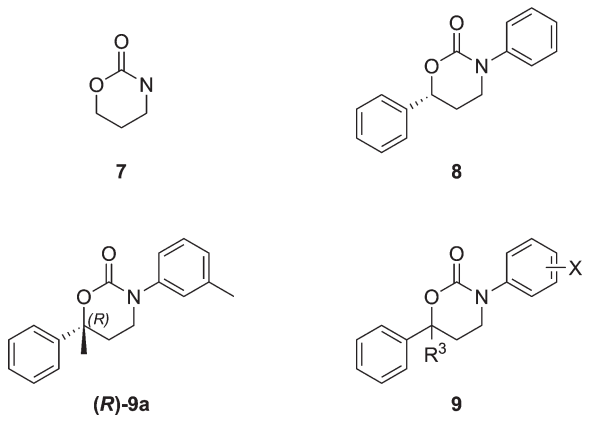

Figure 2. Design of oxazinanone 11β-HSD1 inhibitors.

cycle. In the mouse 11β-HSD1 structure 1Y5R,[35] the side chain hydroxyl groups of Ser170 and Tyr183 both donate hydrogen bonds to the hydroxyl oxygen at C11 of corticosterone, the murine analogue of cortisol. 1n 2BEL, a human 11β-HSD1 structure, Ser170 and Tyr183 donate hydrogen bonds to the ketone and ring E carboxylate of **1**, respectively. 11β-HSD1 has large, primarily hydrophobic pockets on both sides of the key hydrogen-bonding residues, Ser170 and Tyr183. One of these (pocket I) is formed by the cofactor, Thr124, Leu126, and Val180. The second hydrophobic pocket (pocket II) is formed by Leu126, Val180, and Tyr177. In 2BEL, Pocket II has a large opening to solvent due to the truncated C-terminus of the protein construct used for crystallization. Subsequently, a full length dimeric human 11β-HSD1 X-ray structure, 2IRW,[36] was published. This structure revealed that the hydrophobic residues of the C-terminal tail of the second monomer substantially close off pocket II, leaving a much smaller opening to solvent than is present in 2BEL. Our early design work employed 2BEL, but once the more physiologically relevant 2IRW became available, this was adopted.

dx.doi.org/10.1021/jm2005354 |*J. Med. Chem.* 2011, 54, 6050–6062

TEMPLATE DESIGN

The 1,3-oxazinan-2-one ring system **7** was one of a small number of cyclic, carbonyl-containing rings selected as starting templates (Figure 2). Fragment **7** was docked into the binding site of the 2BEL structure of 11β-HSD1 with the carbonyl oxygen of the cyclic carbamate positioned to accept a hydrogen bond from the hydroxyl of Ser170 and the ring oxygen positioned to accept a hydrogen bond from the hydroxyl of Tyr183. This binding mode was suggested by the hydrogen bonding network of the 1,2,4-triazole ligand in fungal SDR structure 1YBV.[37] By use of a proprietary structure based design tool,[38] more than 5000 molecules were grown in silico by adding fragments directly to the N3 and C6 positions of **7**. Diphenyloxazinanone **8** was selected from this set of de novo grown molecules based on its excellent and complementary fit to the binding pocket of the enzyme (Figure 3). In the model of **8**, both the carbonyl oxygen and the ring oxygen remained in good hydrogen bonding distance to the hydroxyl groups of Ser170 and Tyr183. The 3-phenyl substituent enjoyed excellent hydrophobic interactions with the enzyme. However, to achieve a good fit to the enzyme binding site, the 6-phenyl substituent had to adopt an energetically unfavorable pseudoaxial orientation on the oxazinanone ring. To reduce the energetic penalty for the pseudoaxial orientation, we appended a methyl group at the 6-position of the oxazinanone. This methyl group was also expected to block oxidative metabolism at the benzylic position. In addition, to fill pocket II better, we appended a methyl group at the meta position of the 3-phenyl ring. These changes gave compound (*R*)-**9a** which retained the hydrogen bond network to the carbamate oxygens modeled for **8**. The added methyl groups better filled pockets I and II, and an improved fit of the 6-phenyl group within pocket I was observed. Compound **9a** and analogues of general structure **9** were selected for synthesis.

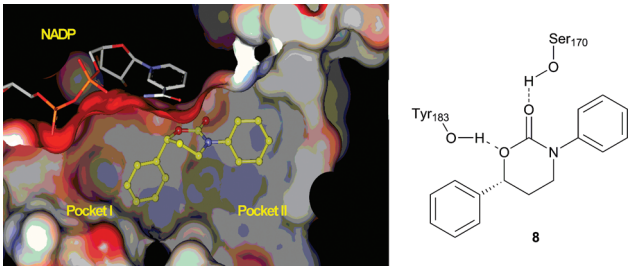

Figure 3. Model of **8** bound to the 2BEL structure of human 11β-HSD1. The second monomer chain is not shown. Ligand **8** interacts with the catalytic site through hydrogen bonds between the carbonyl oxygen and the side chain hydroxyl of Ser170 and between the ring oxygen and the side chain hydroxyl of Tyr183.

Table 1. Aniline SAR

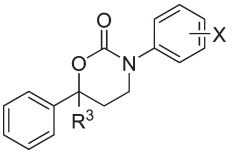

compd	R^3	X	enzyme IC_{50} [a] (nM)
9a	Me	3-Me	42
9a1[b]	Me	3-Me	23
9a2[c]	Me	3-Me	152
9b1[d]	H	3-Me	999
9b2[e]	H	3-Me	353
9c	Me	H	160
9d	Me	2-Cl	40
9e	Me	3-Cl	103
9f	Me	3-Br	23
9g	Me	4-Cl	229
9h	Me	4-CF_3	805
16[f]	Me		631

[a] Average of at least two replicates. [b] Shorter t_R isomer. Stereochemical configuration not assigned. [c] Longer t_R isomer. Stereochemical configuration not assigned. [d] (*R*) isomer. [e] (*S*) isomer. [f] Structure is shown in Scheme 2.

CHEMISTRY

Compounds of general structure **9** (Table 1) were prepared as shown in Scheme 1. Addition of allyl Grignard to acetophenone (**10**) followed by ozonolysis and selective tosylation of the primary alcohol gave hydroxytoslyate **11a**. Enantiopure hydroxytosylates **11b** were prepared from the corresponding commercially available (*R*) and (*S*) enantiomers of **12**. The oxazinanone ring was formed in one pot by treatment of hydroxytosylates **11** with aryl isocyanates in the presence of DBU. The enantiomers of **9a** were separated by HPLC on a chiral column.

N-(4-Bromobenzyl) analogue **16** was prepared as shown in Scheme 2. Hydroxynitrile **13**, prepared by addition of acetonitrile anion to acetophenone (**10**), was reduced with borane to amino

Scheme 1. Synthesis of Analogues 9[a]

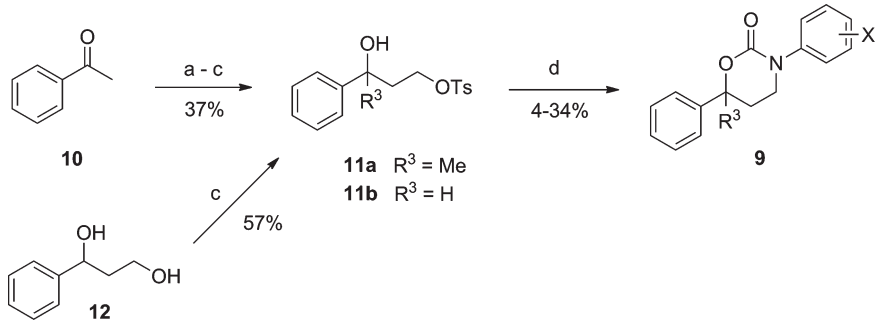

[a] See Table 1 for definitions of R^3 and X. Reagents and conditions: (a) $H_2C{=}{=}CHCH_2MgBr$, THF, −70 °C to room temp; (b)O_3, CH_2Cl_2, −70 °C, then $NaBH_4$, −20 °C; (c)TsCl, Et_3N, CH_2Cl_2, 0 °C to room temp; (d) X-C_6H_4NCO, DBU, THF, CH_2Cl_2, 0 °C to room temp.

dx.doi.org/10.1021/jm2005354 |*J. Med. Chem.* 2011, 54, 6050–6062

Scheme 2. Synthesis of 16[a]

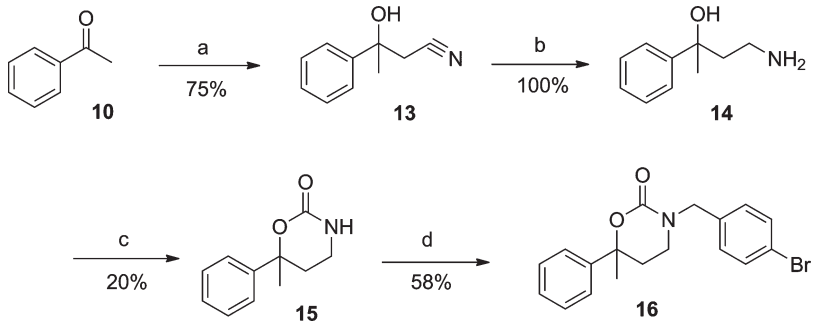

[a] Reagents and conditions: (a)MeCN, *n*-BuLi, THF, −20 °C to room temp; (b) $BH_3 \cdot Me_2S$, THF, reflux, 16 h; (c) triphosgene, Et_3N, CH_2Cl_2, 0 °C, 1 h; (d) 4-bromobenzyl bromide, NaH, THF, room temp, 16 h.

Scheme 3. Synthesis of Analogues 18[a]

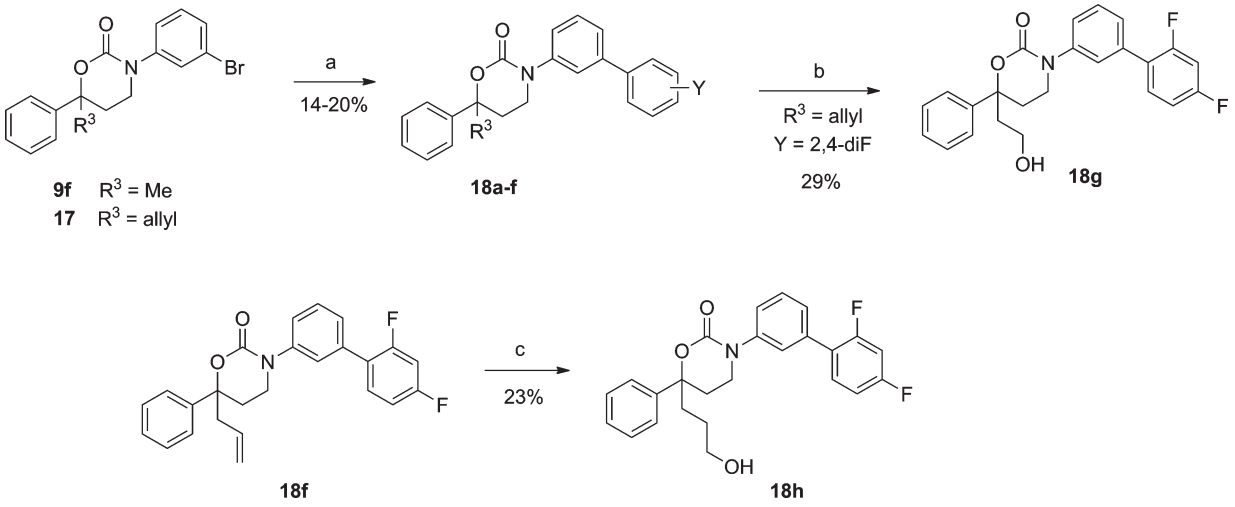

[a] See Table 3 for definitions of R^3 and Y. Reagents and conditions: (a) Y-$PhB(OH)_2$, $Pd(PPh_3)_2Cl_2$, $NaHCO_3$, H_2O, THF, reflux; (b) O_3, CH_2Cl_2, −78 °C, then $NaBH_4$, −20 °C to room temp; (c) $BH_3 \cdot$THF, 0 °C to room temp, then $NaBO_3 \cdot H_2O$, H_2O, 0 °C to room temp.

Scheme 4. Synthesis of Intermediate 17[a]

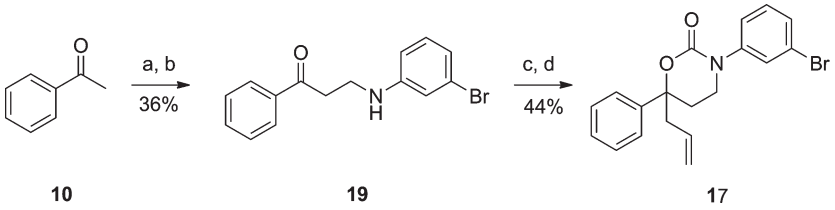

[a] Reagents and conditions: (a) Me_2NH, HCHO, HCl, EtOH, 70 °C, 16 h; (b) 3-Br-$C_6H_3NH_2$, 1:1 H_2O/EtOH, 80 °C, 16 h; (c) MeOCOCl, K_2CO_3, THF, 0 °C to room temp, 2 h; (d) $H_2C{=}CHCH_2MgBr$, THF, −70 °C to room temp, 2 h.

alcohol **14**. Treatment of **14** with triphosgene afforded oxazinanone **15** which was N-alkylated with 4-bromobenzyl bromide to give **16**.

Compounds of general structure **18** (Table 3) were prepared as shown in Scheme 3. Starting bromide **9f** was prepared as shown in Scheme 1, while **17** was accessed as shown in Scheme 4. Suzuki coupling of fluorophenylboronic acids with **9f** and **17** afforded **18a**−**f**. The allyl R^3 substituent of compound **18f** was converted to a 2-hydroxyethyl group in **18g** by ozonolysis and borohydride reduction. Hydroboration effected the conversion of the allyl R^3 substituent in **18f** to the 3-hydroxypropyl substituent in **18h**. The enantiomers of two compounds, **18d** and **18h**, were separated by preparative SFC on a chiral column.

Bromides **22** (Scheme 5) were used as key intermediates to access analogues of general structure **25** (Table 4). Reaction of 3-chloropropiophenones **20** with allyl Grignard in the presence of $CeCl_3$ gave chloro alcohols **21**, which were treated with (*S*)-4-bromo-α-methylbenzyl isocyanate to give bromooxazinanones **22** as mixtures of diastereomers. Suzuki coupling of

dx.doi.org/10.1021/jm2005354 |*J. Med. Chem.* 2011, 54, 6050–6062

Scheme 5. Synthesis of Biphenylethyl Analogues 25[a]

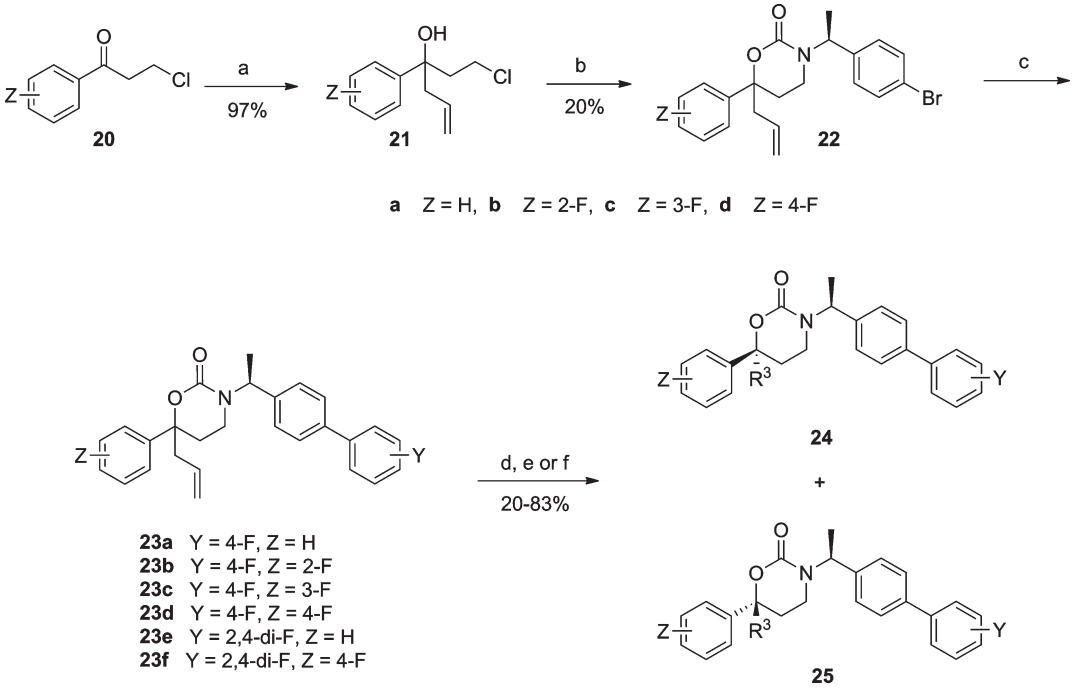

[a] Definitions of R^3, Y, and Z in **25** are given in Table 4. Reagents and conditions: (a) $H_2C{=}CHCH_2MgBr$, $CeCl_3$, THF, −78 °C to room temp, 16 h; (b) (*S*)-4-Br-$C_6H_4CHMeNCO$, DBU, THF, reflux, 1 day; (c) Y-$C_6H_5B(OH)_2$, $(PPh_3)_2PdCl_2$, Na_2CO_3, H_2O, THF; (d) O_3, CH_2Cl_2, −78 °C, then $NaBH_4$, −20 °C to room temp; (e) $NaIO_4$, OsO_4, 1:1 H_2O/THF, room temp, 2 h, then $NaBH_4$, MeOH, room temp, 1 h; (f) $BH_3 \cdot$THF, 0 °C to room temp, then $NaBO_3 \cdot H_2O$, H_2O, 0 °C to room temp.

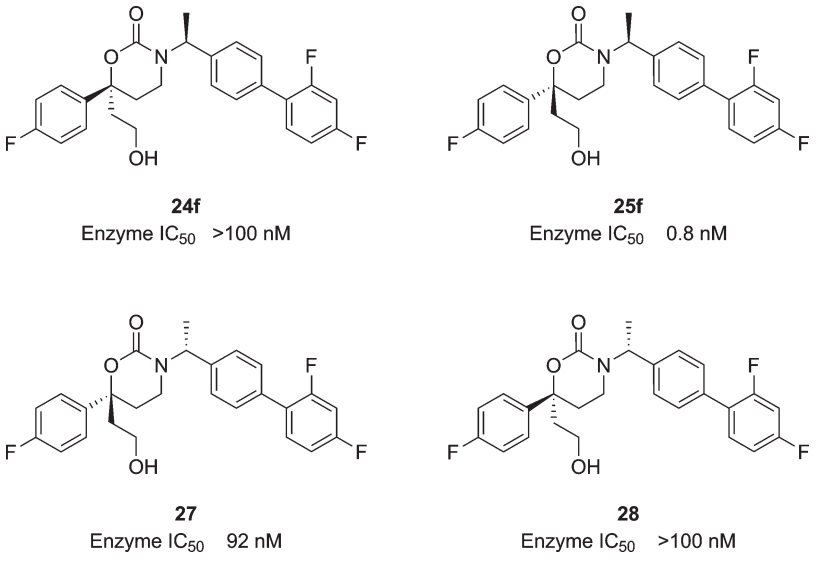

Figure 4. Diastereomers of **25f**.

bromooxazinanones **22** with 4-fluoro and 2,4-difluorophenylboronic acids afforded biphenyl intermediates **23**. The allyl side chains were elaborated to the 2-hydroxyethyl and 3-hydroxypropyl side chains, as described above for **18g** and **18h**, to give diastereomeric products **24** and **25**. Compound **25e** (Table 4), with an ethyl group at the benzylic position, was prepared by an analogous sequence using (*S*)-4-Br$C_6H_4CHEtNCO$ in the second step. In one case (**25k**), the allyl group of bromo intermediate **23d** was elaborated to 2-hydroxyethyl prior to Suzuki coupling. The desired, potent compounds **25** were readily separated from the undesired diastereomers **24** by chromatography on silica gel. Separation of the diastereomers of **22** and **23** on silica gel could also be achieved routinely. In all cases, the potent diastereomers **25**, and the diastereomers of precursors **22** and **23** that could be converted to **25**, were characterized by a consistent downfield shift of the benzylic methyl doublet (∼1.5 ppm) in the ^{1}H NMR

dx.doi.org/10.1021/jm2005354 |*J. Med. Chem.* 2011, 54, 6050–6062

Scheme 6. Elaboration of 2-Hydroxyethyl to Other Two-Carbon Side Chains[a]

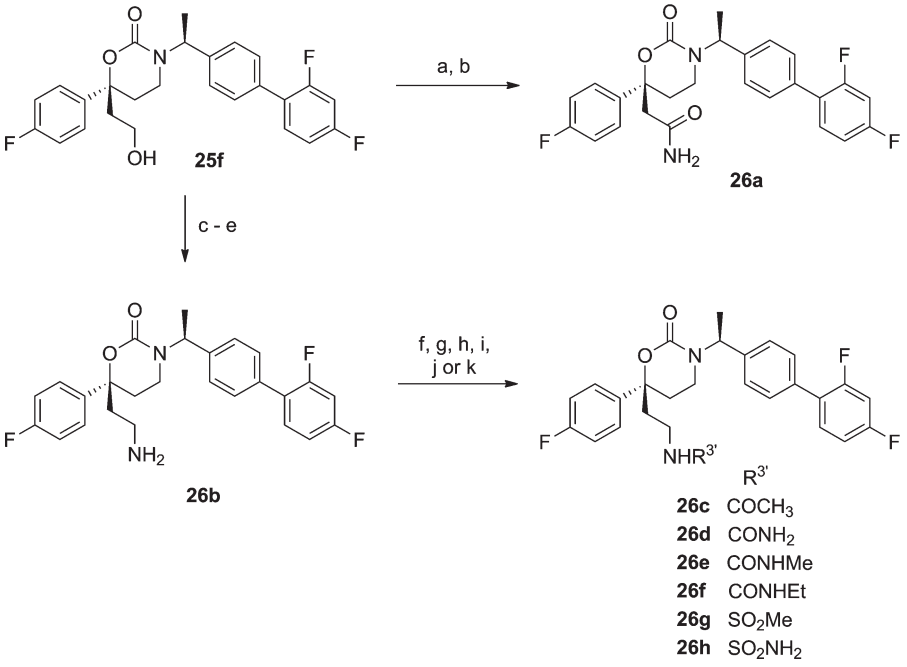

[a] Reagents and conditions: (a) Jones reagent, Me_2CO, 0 °C to room temp, 16 h; (b) NH_3, EDC, HOBt, *i*-Pr_2NEt, CH_2Cl_2, room temp, 16 h; (c) MsCl, Et_3N, CH_2Cl_2, 0 °C to room temp, (d) NaN_3, DMF, 70 °C, 16 h; (e) PPh_3, 20:1 THF/H_2O, room temp, 16 h; (f) Ac_2O, NaOAc, room temp, 2 h; (g) H_2CONH_2, HCl, H_2O, reflux, 16 h; (h) $MeNH_2$, CDI, *i*-Pr_2NEt, CH_2Cl_2, room temp, 16 h; (i) $EtNH_2$, CDI, *i*-Pr_2NEt, CH_2Cl_2, room temp, 16 h; (j) $MeSO_2Cl$, Et_3N, CH_2Cl_2, room temp, 2 h; (k) $H_2NSO_2NH_2$, dioxane, reflux, 16 h.

Scheme 7. Elaboration of 3-Hydroxypropyl to Other Three-Carbon Side Chains[a]

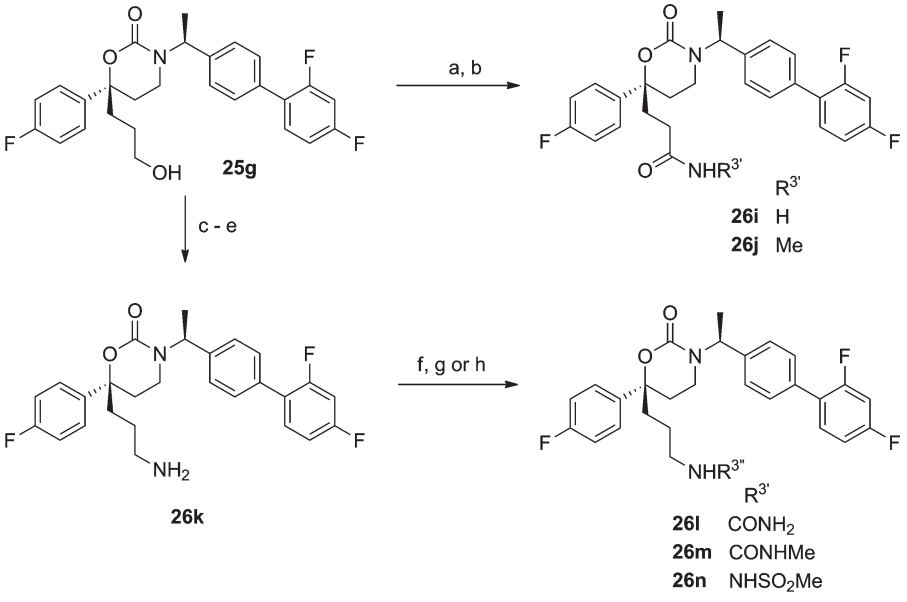

[a] Reagents and conditions: (a) Jones reagent, Me_2CO, 0 °C to room temp, 16 h; (b) $R^{3'}NH_2$, EDC, HOBt, *i*-Pr_2NEt, CH_2Cl_2, room temp, 16 h; (c) MsCl, Et_3N, CH_2Cl_2, 0 °C to room temp; (d) NaN_3, DMF, 70 °C, 16 h; (e) PPh_3, 20:1 THF/H_2O, room temp, 16 h; (f) H_2CONH_2, HCl, H_2O, reflux, 16 h; (g) $MeNH_2$, CDI, *i*-Pr_2NEt, CH_2Cl_2, room temp, 16 h; (h) $MeSO_2Cl$, Et_3N, CH_2Cl_2, room temp, 2 h.

spectrum compared to the same resonance in **24** (~1.2 ppm). The absolute configuration of **25f** (Table 4) was established by X-ray crystallography, and the configurations of other analogues were assigned based on the ^1H NMR chemical shift of the benzylic methyl doublet. Compounds **27** and **28** (Figure 4), the enantiomers of **24f** and **25f**, were prepared by the sequence shown in Scheme 5 using (*R*)-4-bromo-α-methylbenzyl isocyanate in the second step.

dx.doi.org/10.1021/jm2005354 |*J. Med. Chem.* 2011, 54, 6050–6062

The syntheses of analogues **26** (Table 5) in which the 2-hydroxyethyl or 3-hydroxypropyl side chains in **25f** and **25g** were further elaborated are depicted in Schemes 6 and 7, respectively. Oxidation of alcohols **25f** and **25g** to carboxylic acids followed by amide formation afforded **26a**, **26i**, and **26j**. Alcohols **25f** and **25g** were converted to the corresponding primary amines **26b** and **26k** which were used to access a number of acylated derivatives (**26c**−**h**, Scheme 6; **26l**−**n**, Scheme 7).

BIOLOGICAL ASSAYS

Compounds were assayed for inhibition of 11β-HSD1 in enzyme- and cell-based assays. Both assays measured the conversion of [^{3}H]cortisone to [^{3}H]cortisol, which was quantified using SPA beads and a microscintillation plate reader.[39] Enzyme assays used recombinant 11β-HSD1 isolated as a microsomal preparation from CHO cells. Assays were performed in 25 mM HEPES, pH 7.4, 50 mM KCl, 2.5 mM NaCl, 1 mM $MgCl_2$, 1 mM NADPH, and 80 nM [^{3}H]cortisone at room temperature for 1 h. Cell-based potency was assessed in differentiated human adipocytes by the addition of cortisone (80 nM [^{3}H]cortisone). Cells were incubated at 37 °C for 2 h, and [^{3}H]cortisol production was quantitated by HPLC. IC_{50} values represent the mean of at least duplicate assays and were generated from an eight-point concentration−response curve.

Table 2. Rat PK Data[a]

compd	po $AUC_{(inf)}$ (ng·h/mL)	po $t_{1/2}$ (h)	iv CL (mL/(min·kg))	F (%)
9a1[b]	99	0.8	71	4
18g1[c]	1045	4.7	71	44
25b[d]	915	3.6	48	19
25d[d]	450	1.6	86	23
25f[e]	3870	3.0	41	94
25k[d]	3168	3.3	44	83

[a] iv dose of 2 mg/kg, po dose of 10 mg/kg. [b] po vehicle: 10% ethanol/10% Tween 80/80% PEG 400 (solution). [c] po vehicle: 1% DMSO qs with 10% ethanol/10% Tween 80/80% PEG 400 (solution). [d] po vehicle: 0.5% methyl cellulose in deionized water (homogeneous suspension). [e] 10% ethanol/10% polysorbate 80/80% PEG 400 (solution).

RESULTS AND DISCUSSION

Designed compound **9a** had enzyme and adipocyte IC_{50} of 42 and 166 nM as a racemate. The enantiomers of **9a** were separated by chiral chromatography, and isomer **9a1** was substantially more potent than **9a2**. The absolute configuration of **9a1** was not determined. The importance of the methyl group at the 6-position of the oxazinanone ring, introduced to favor the desired pseudoaxial conformation of the 6-phenyl ring in pocket I, was demonstrated by preparation of **9b1** and **9b2**, both of which were less potent than **9a1**. Substitution on the *N*-phenyl ring was briefly examined. Deletion of the methyl group at the meta-position decreased potency (**9c** versus **9a**). Introduction of chlorine at the ortho-position (**9d**) or bromine at the meta-position (**9f**) restored potency levels comparable to that of **9a**, while chlorine substitution at the para-position (**9g**) was unfavorable. A rat PK study showed that **9a1** had low oral bioavailability and was subject to rapid clearance (Table 2).

Inspection of a model of **9a** bound to 11β-HSD1[38] suggested that the *m*-methyl group of **9a** could be replaced with a phenyl ring to give **18a** which was expected to better fill hydrophobic pocket II. With an enzyme IC_{50} of 4.7 nM, compound **18a** (Table 3) was 9× more potent than **9a**. The adipocyte potency of **18a** exhibited a 2.5× improvement over that of **9a**; however, its $t_{1/2}$ in rat liver microsomes (RLM $t_{1/2}$) was only 16 min. Introduction of fluorine substituents on the aromatic rings was expected to improve metabolic stability. In fact, fluorine (Table 3) and other small lipophilic substituents (data not shown) were generally tolerated on the distal ring of the biphenyl system, and fluorine in the para position (**18d**) increased the RLM $t_{1/2}$ to >60 min. The 2,4-difluoro substitution in **18e** proved to be especially favorable with

Table 3. Biphenyl SAR

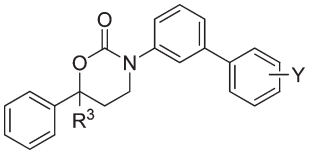

compd	R^3	Y	enzyme IC_{50}[a] (nM)	adipocyte IC_{50}[a] (nM)	RLM $t_{1/2}$ (min)
18a	Me	H	4.7	64	16
18b	Me	2-F	12	40	
18c	Me	3-F	4.2	50	
18d	Me	4-F	3.3		62
18d1[b]	Me	4-F	3.3	36	
18d2[c]	Me	4-F	29		
18e	Me	2,4-di-F	1.6	24	75
18f	CH_2=$CHCH_2$	2,4-di-F	3.2	50	
18g	$HOCH_2CH_2$	2,4-di-F	1.2	4.4	
18g1[d]	$HOCH_2CH_2$	2,4-di-F	0.8	1.9	47
18g2[e]	$HOCH_2CH_2$	2,4-di-F	140	570	
18h	$HOCH_2CH_2CH_2$	2,4-di-F	4.4	6.9	

[a] Average of at least two replicates. [b] Longer t_R isomer on a ChiralCel-AS column. [c] Shorter t_R isomer on a ChiralCel-AS column. [d] Longer t_R isomer on a Chiralpak IA column. [e] Shorter t_R isomer on a Chiralpak IA column.

dx.doi.org/10.1021/jm2005354 |J. Med. Chem. 2011, 54, 6050–6062

Table 4. SAR of Biphenylmethyl Analogues 25

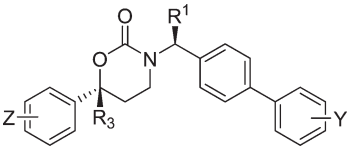

compd	R^1	R^3	Y	Z	enzyme IC_{50}[a] (nM)	adipocyte IC_{50}[a] (nM)	enzyme/plasma IC_{50} (nM)	CYP3A4 IC_{50}[a] (μM)	RLM $t_{1/2}$ (min)
25a	Me	CH_2CH_2OH	2,4-di-F	H	0.7	0.9	8.4		16
25b	Me	$CH_2CH_2CH_2OH$	2,4-di-F	H	0.6	0.7	17.9	14	18
25c	Me	CH_2CH_2OH	4-F	H	0.5	0.8	5.7		28
25d	Me	$CH_2CH_2CH_2OH$	4-F	H	0.6	0.4	11.9	11	28
25e	Et	$CH_2CH_2CH_2OH$	4-F	H	0.6	0.9	18.7	1.5	>60
25f	Me	CH_2CH_2OH	2,4-di-F	4-F	0.8	2.5	17.5	12	119
25g	Me	$CH_2CH_2CH_2OH$	2,4-di-F	4-F	1.1	2.1	18.0	>30	21
25h	Me	$CH_2CH_2CH_2OH$	4-F	2-F	0.9	1.2	8.6	6	32
25i	Me	$CH_2CH_2CH_2OH$	4-F	3-F	0.9	1.3	11.8	7	63
25j	Me	$CH_2CH_2CH_2OH$	4-F	4-F	0.6	0.7	14.7	8	29
25k	Me	CH_2CH_2OH	4-F	4-F	0.5	1.5	18.5	21	58

[a] Average of at least two replicates.

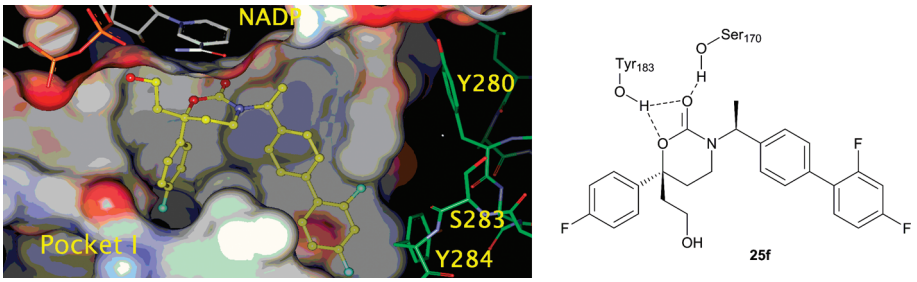

Figure 5. Model of **25f** bound to the 2IRW structure of human 11β-HSD1. The side chain hydroxyl of Ser170 forms a hydrogen bond to the carbonyl oxygen of the ligand, while the phenolic hydroxyl of Tyr183 lies within hydrogen bonding distance of both the carbonyl and ring oxygen atoms of the ligand. The primary alcohol of the ligand forms a hydrogen bond to a phosphate oxygen of NADP. The 4-fluorophenyl ring stacks with Tyr183, and its para carbon fits into a hydrophobic subpocket formed by Thr124, Ser125, Leu126, and Val180. The 2,4-difluorophenyl ring interacts with the Tyr284 side chain of the partner chain in this model.

enzyme and adipocyte potencies 3× better than **18a**. Despite the attractive potency of **18e**, its hydrophobicity (alogP > 5; PSA = 30 Å^2) was outside the desirable range for druglike molecules.

Two approaches were explored to reduce hydrophobicity by introduction of polar functionality groups. First, a library of 34 analogues of general structure **18** with polar Y substituents was prepared by coupling commercially available boronic acids to **9f**. As predicted by our model, polar Y substitutuents were not tolerated (data shown in Supporting Information).

The second approach resulted from examination of a model of (*R*)-**18e** bound to the protein. This model suggested the possibility of forming hydrogen bonds to the pyrophosphate portion of the NADP cofactor using the 6-methyl substituent on the oxazinanone ring as an attachment point. Models suggested that replacement of the methyl group with a 2-hydroxyethyl ((*S*)-**18g**) or 3-hydroxypropyl ((*R*)-**18h**) moiety would position a hydroxyl group within hydrogen bonding distance of the NADP cofactor pyrophosphate. These compounds were prepared as their racemates. The 2-hydroxyethyl compound **18g** retained the enzyme potency of **18e**, while **18h** was 2.5× less potent. In the adipocyte assay, both **18g** and **18h** were markedly more potent than **18e**. The isomers of **18g** were separated by chromatography on a chiral column, and isomer **18g1** was shown to be responsible for the activity of **18g**. In a rat PK study, **18g1** demonstrated substantially greater exposure than **9a1**, although it remained subject to high clearance (Table 2). The calculated physical properties of **18g1** (alogP = 4.6; PSA = 50 Å^2) were more favorable than those of **18e**.

Despite its improved physical properties and PK profile, the aniline functionality of **18g1** was considered undesirable in a chronically administered drug.[40,41] Replacement of the *N*-phenyl group with an *N*-benzyl group was investigated. Examination of a model of **16** suggested that an (*S*)-methyl group at the benzylic carbon would gain hydrophobic interactions but that transposition of the distal phenyl ring from the meta to para position would be necessary to properly occupy pocket II.

Thus, **25a** and **25b**, (*S*)-α-methylbenzyl analogues of **18g** and **18h**, were prepared and exhibited excellent enzyme and cell potencies (Table 4). The 3-hydroxypropyl compound **25b** suffered a greater loss in potency in the presence of human plasma than **25a**. Analogues **25c** and **25d**, in which the Y substitutuent was

dx.doi.org/10.1021/jm2005354 |*J. Med. Chem.* 2011, 54, 6050–6062

Table 5. Side Chain SAR

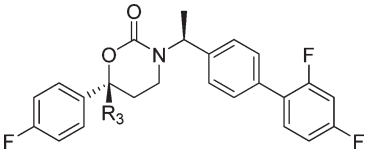

compd	R^3	enzyme IC_{50} [a] (nM)	adipocyte IC_{50} [a] (nM)	enzyme/plasma IC_{50} [a] (nM)	CYP3A4 IC_{50} [a] (μM)	RLM $t_{1/2}$ (min)
25f	CH_2CH_2OH	0.8	2.5	18	12	119
26a	CH_2CONH_2	2.8	12	62	>30	
26b	$CH_2CH_2NH_2$	2.7	66		3	
26c	CH_2CH_2NHAc	7.1	34	164		
26d	$CH_2CH_2NHCONH_2$	0.8	3.5	29	5	
26e	$CH_2CH_2NHCONHMe$	3.1	16		1	
26f	$CH_2CH_2NHCONHEt$	22	69			
26g	$CH_2CH_2NHSO_2Me$	1.0	9.0	45	9	
26h	$CH_2CH_2NHSO_2NH_2$	2.0	11	37	12	
25g	$CH_2CH_2CH_2OH$	1.1	2.0	18	>30	21
26i	$CH_2CH_2CONH_2$	1.0	5.0	42	>30	25
26j	$CH_2CH_2CONHMe$	22	145			
26k	$CH_2CH_2CH_2NH_2$	5.7	16		2	
26l	$CH_2CH_2CH_2NHCONH_2$	1.4	19	53	4	
26m	$CH_2CH_2CH_2NHCONHMe$	4.1	19		0.6	
26n	$CH_2CH_2CH_2NHSO_2Me$	1.8	3.7	32	7	>60

[a] Average of at least two replicates.

changed from 2,4-difluoro to 4-fluoro, showed similar trends. Changing the R^1 substituent from methyl to ethyl increased both plasma shift and CYP3A4 inhibition (**25e** versus **25d**). Introduction of a 4-fluoro substituent on the left-hand phenyl ring gave **25f** and **25g**, both of which had excellent enzyme and cell potency, combined with limited CYP3A4 inhibition. Hydroxyethyl compound **25f** was distinguished by its superior metabolic stability in rat liver microsomes. Analogues of **25d** with fluoro substitution at the 2-position (**25h**), 3-position (**25i**), and 4-position (**25j**) on the left-hand phenyl ring all had excellent potency but had IC_{50} < 10 μM against CYP3A4. Introduction of a 4-fluoro substituent onto the left-hand phenyl ring of **25c** raised the CYP3A4 IC_{50} above 10 μM and gave **25k** with good RLM stability. Rat PK parameters were determined for **25b**, **25d**, **25f**, and **25k**. The monofluoro, 3-hydroxypropyl analogue **25d** demonstrated the highest clearance (Table 2). Both 2-hydroxyethyl compounds, **25f** and **25k**, possessed excellent oral bioavailability.

Protein-bound models of **25f** (Figure 5) and **25g** indicated that other functional groups capable of donating a hydrogen bond to the cofactor pyrophosphate would be accommodated within the protein binding site. Table 5 shows that certain analogues of this type retained enzyme IC_{50} < 5 nM; however, in no case did the adipocyte potencies of these compounds exceed those of **25f** and **25g**. Furthermore, with the exception of primary amides **26a** and **26i**, these compounds were more potent inhibitors of CYP3A4 than **25f** and **25g**.

Compounds **24f**, **27**, and **28**, the three diastereomers of **25f**, were much less potent than **25f** (Figure 4), supporting the validity of our model.

Profile of 25f. Compound **25f** was selected for further in vitro and in vivo characterization. The compound displayed >1000× selectivity for 11β-HSD1 over three related hydroxysteroid dehydrogenases, three CYP isozymes, hERG, and three nuclear receptors (MR, FXR, and GR) (Table 6). Among this group

Table 6. In Vitro Characterization of 25f

enzyme/receptor	IC_{50} (μM)
11β-HSD2[a]	>10
17β-HSD1[b]	>10
3β-HSD2[c]	4.7
CYP3A4[d]	>10
CYP2D6[d]	>10
CYP2C9[d]	4.9
hERG[e]	>10
receptor	**EC_{50} (μM)**
FXR[f]	>10
GR[g]	>10
MR[h]	>5

[a] Compounds were diluted in DMSO and dispensed to 96-well microtiter plates. Substrate (35 mM 3H-cortisol and 1 mM NAD^+ in 50 mM potassium phosphate buffer, pH 7.4) and microsomes isolated from CHO cells overexpressing 11B-HSD2 were added, and the plate was incubated at room temperature for 60 min. The reaction was quenched with ACN, and cortisone product was detected by HPLC. [b] Puranen, T.; Poutanen, M.; Ghosh, D.; Vihko, P.; Vihko, R. *Mol. Endocrinol.* **1997**, *11*, 77. [c] Frye, S. V.; Haffner, C. D.; Maloney, P. R.; Mook, R. A.; Dorsey, G. F.; Hiner, R. N.; Cribbs, C. M.; Wheeler, T. N.; Ray, J. A. *J. Med. Chem.* **1994**, *37*, 2352. [d] Assay kit was purchased from Invitrogen. [e] Assay was performed by MDS Pharma Services. [f] Parks, D. J.; Blanchard, S. G.; Bledsoe, R. K.; Chandra, G.; Consler, T. G.; Kliewer, S. A.; Stimmel, J. B.; Willson, T. M.; Zavacki, A. M.; Moore, D. D.; Lehmann, J. M. *Science* **1999**, *284*, 1365. [g] Assay kit was purchased from Panvera/Invitrogen. [h] Grover, G. S.; Turner, B. A.; Parker, C. N.; Meier, J.; Lala, D. S.; Lee, P. H. *J. Biomol. Screening* **2003**, *8*, 239.

dx.doi.org/10.1021/jm2005354 |*J. Med. Chem.* 2011, 54, 6050–6062

Table 7. Pharmacokinetics of 25f in Three Species

species	dose iv/po (mg/kg)	$AUC_{(inf)}$ (ng·h/mL)	$t_{1/2}$ (h)	iv CL (mL/(min·kg))	F (%)
rat	2/10[a]	3870	3.0	41	94
dog	1/2[b]	584	3.7	9.2	16
monkey	1/2[b]	1500	10.9	5.8	26

[a] po vehicle:10% ethanol/10% polysorbate 80/80% PEG 400 (solution). [b] po vehicle: 0.5% methylcellulose in deionized water.

Table 8. Mouse Tissue Distribution of 25f[a]

	drug level (ng/mL)		
time (h)	liver	adipose	plasma
1	15317	5519	5927
4	9813	3165	3260
8	1898	632	573

[a] Animals (n = 3) were dosed po with 30 mg/kg dissolved in 10% ethanol/10% Tween 80/80% PEG 400. Tissues were collected upon sacrifice at 1, 4, and 8 h and snap frozen. Later, thawed tissues were homogenized in 0.05 M BES, pH 7, and compound was extracted into acetonitrile. Concentrations were determined by LC−MS/MS by comparison to a standard curve generated independently in each tissue matrix.

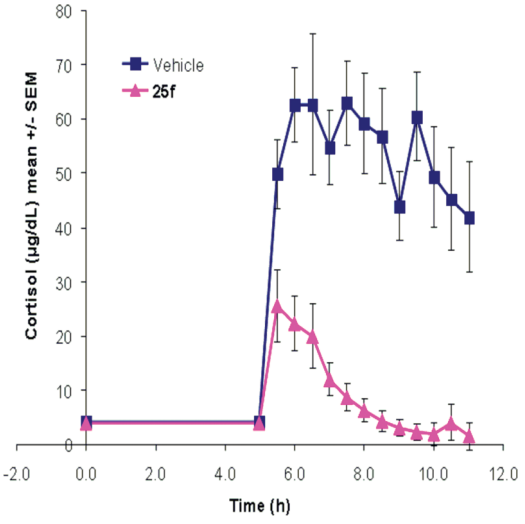

Figure 6. Pharmacodynamic effects of **25f** in cynomolgus monkeys. Animals were dosed with dexamethasone 8 h prior to compound administration (t = −8 h) to suppress endogenous plasma cortisol concentrations. The animals received vehicle or compound (10 mg/kg, po) at time zero (t = 0 h) and 5 h later (t = 5 h) and were challenged with cortisone 21-acetate (25 mg, po). Blood samples were drawn every 30 min for 6 h to measure cortisol production. The animals were crossed over after a 7-day washout.

of antitargets, IC_{50} values for 3β-HSD2 and CYP2C9 of 4.7 and 4.9 μM were determined. Profiling against 165 enzymes and receptors (MDS PanLabs Spectrum Screen) showed **25f** to be >5000× selective over all targets tested. The compound is >99% protein bound in dog, monkey, and human plasma, consistent with a pronounced shift in enzyme potency when assayed in the presence of 50% human plasma. **25f** was stable in rat liver microsomes and was bioavailable in rat and to a lesser extent in dog and monkey (Table 7). When dosed orally at 30 mg/kg to mice, **25f** was distributed into adipose and liver, key target tissues for the inhibition of 11β-HSD1 (Table 8).

In Vivo Biology. The poor potency of **25f** against mouse 11β-HSD1 (IC_{50} = 670 nM) precluded the use of rodent pharmacodynamic models. However, the compound was equally potent against 11β-HSD1 from cynomolgus monkeys (IC_{50} = 0.97 nM), and this species was selected to measure in vivo inhibition of 11β-HSD1. In this model, endogenous plasma glucocorticoids were suppressed with dexamethasone, and the animals were challenged with a bolus of cortisone 21-acetate 5 h after compound administration. A single 10 mg/kg dose of **25f**, administered by oral gavage, reduced cortisol production ~85% (Figure 6), consistent with substantial inhibition of 11β-HSD1 in vivo.

CONCLUSION

We have described the structure-based design of a novel class of 11β-HSD1 inhibitors built around a 1,3-oxazinan-2-one ring. Optimization (Figure 7) furnished **25f** which combined excellent potency against 11β-HSD1 in human adipocytes with >1000× selectivity over three other hydroxysteroid dehydrogenases, including 11β-HSD2. This compound was orally bioavailable in three species and distributed to adipose tissue in mouse. Oral administration to cynomolgus monkeys substantially reduced plasma cortisol levels following a cortisone challenge.

EXPERIMENTAL SECTION

1-Chloro-3-(4-fluorophenyl)hex-5-en-3-ol (21d). A 250 mL flask was charged with anhydrous $CeCl_3$ (5.58 g, 22.6 mmol) and THF (40 mL). The mixture was vigorously stirred for 3.5 h at room temperature. The suspension was cooled to −78 °C, and a solution of allylmagnesium bromide (1.0 M in THF, 21 mL, 21.0 mmol) was added. After the mixture was stirred for 2 h at −78 °C, a solution of 3-chloro-1-(4-fluorophenyl)propan-1-one (2.52 g, 13.5 mmol) in THF (30 mL) was added via cannula. The reaction mixture was allowed to slowly warm to 8 °C while stirring overnight (18 h). The reaction was quenched with saturated aqueous $NaHCO_3$, and the aqueous layer was extracted with EtOAc. The organic layer was dried over Na_2SO_4. After the solvents were evaporated, the residue was purified by chromatography on silica gel, eluting with hexanes/EtOAc to afford **21d** (3.00 g, 97%) as an oil. ^{1}H NMR (400 MHz, $CDCl_3$) δ 7.37−7.32 (m, 2H), 7.07−7.02 (m, 2H), 5.57−5.47 (m, 1H), 5.20−5.19 (m, 1H), 5.16 (m, 1H), 3.59−3.52 (m, 1H), 3.24−3.18 (m, 1H), 2.70 (dd, J = 13.8, 5.9 Hz, 1H), 2.50 (dd, J = 13.8, 8.5 Hz, 1H), 2.29 (t, J = 7.9 Hz, 2H), 2.22 (s, 1H); ^{19}F NMR (376 MHz, $CDCl_3$) δ −116.52 (m); LC−MS method 1, t_R = 1.79 min, m/z 213, 211 $(M - OH)^+$.

6-Allyl-3-((*S*)-1-(4-bromophenyl)ethyl)-6-(4-fluorophenyl)-1,3-oxazinan-2-one (22d). A mixture of **21d** (0.413 g, 1.8 mmol, 1.0 equiv), (*S*)-(−)-1-(4-bromophenyl)ethyl isocyanate (0.501 g, 2.2 mmol, 1.2 equiv), and DBU (0.738 g, 4.8 mmol, 2.7 equiv) in THF (10 mL) was heated at reflux for 25 h. The mixture was diluted with EtOAc and washed with 1 N aqueous HCl. The aqueous phase was extracted with EtOAc (2×). The combined organic phase was dried over Na_2SO_4. After the solvents were evaporated, the crude product was directly used in the next step without further purification.

A portion of the crude product was purified by chromatography on silica gel, eluting with hexanes/EtOAc to afford analytical samples.

(*R*)-6-Allyl-3-((*S*)-1-(4-bromophenyl)ethyl)-6-(4-fluorophenyl)-1,3-oxazinan-2-one (*RS*)-22d. ^{1}H NMR (400 MHz, $CDCl_3$) δ 7.25−7.20 (m, 4H), 7.05−7.01 (m, 2H), 6.71 (d, J = 8.5 Hz, 2H), 5.74−5.64 (m, 1H), 5.58 (q, J = 7.0 Hz, 1H), 5.09−4.99 (m, 2H), 2.92−2.87 (m, 1H), 2.63−2.50 (m, 2H), 2.33−2.16 (m, 3H), 1.47

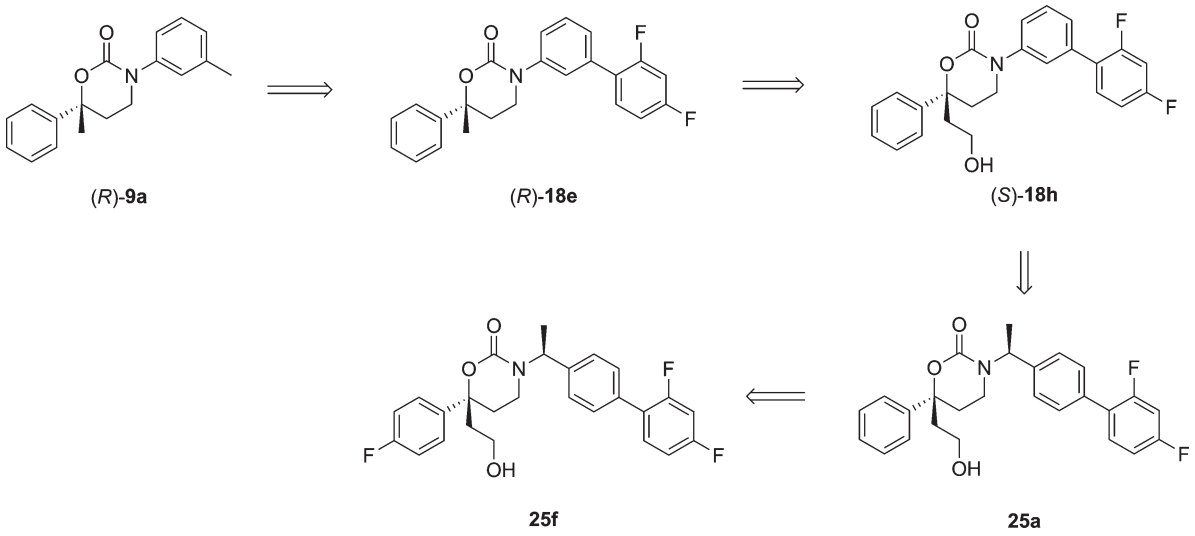

Figure 7. Evolution of **25f** from (*R*)-**9a**.

(d, *J* = 7.0 Hz, 3H); ^{19}F NMR (376 MHz, $CDCl_3$) δ −114.91 (m). LC−MS method 1, t_R = 9.71 min, *m*/*z* = 418, purity = 86%. Anal. Calcd for $C_{21}H_{21}BrFNO_2$: C, 60.30; H, 5.06; N, 3.35. Found: C, 60.25; H, 4.87; N, 3.24.

(*S*)-6-Allyl-3-((*S*)-1-(4-bromophenyl)ethyl)-6-(4-fluorophenyl)-1,3-oxazinan-2-one (*SS*)-22d. ^{1}H NMR (400 MHz, $CDCl_3$) δ 7.46 (d, *J* = 8.2 Hz, 2H), 7.31−7.28 (m, 2H), 7.17 (d, *J* = 8.2 Hz, 2H), 7.07 (t, *J* = 8.5 Hz, 2H), 5.76−5.66 (m, 2H), 5.10−4.99 (m, 2H), 2.75−2.52 (m, 4H), 2.23−2.19 (m, 1H), 2.08−2.00 (m, 1H), 1.24 (d, *J* = 7.0 Hz, 3H); ^{19}F NMR (376 MHz, $CDCl_3$) δ −115.07 (m); LC−MS method 2, t_R = 2.03 min, *m*/*z* 420, 418 (MH^+).

6-Allyl-3-((*S*)-1-(2′,4′-difluoro-[1,1′-biphenyl]-4-yl)ethyl)-6-(4-fluorophenyl)-1,3-oxazinan-2-one (23f). A mixture of **22d** (10.0 g, 24.0 mmol), 2,4-difluorophenylboronic acid (4.74 g, 28.7 mmol), $PdCl_2(PPh_3)_2$ (672 mg, 0.96 mmol), 2 M aqueous Cs_2CO_3 (30 mL, 600 mmol), and dioxane (120 mL) was heated at reflux under N_2 for 2 h. The mixture was cooled to room temperature and filtered. The filtrate was extracted with EtOAc (3×). The combined organic layer was washed with brine, dried over Na_2SO_4, and concentrated to afford crude **23f** which was used in the next step without further purification. A portion of the crude product was purified by chromatography on silica gel, eluting with hexanes/EtOAc to provide analytical samples.

(*S*)-6-Allyl-3-((*S*)-1-(2′,4′-difluorobiphenyl-4-yl)ethyl)-6-(4-fluorophenyl)-1,3-oxazinan-2-one (*SS*)-23f. ^{1}H NMR ($CDCl_3$) δ 7.47 (d, *J* = 8.2 Hz, 2H), 7.42−7.30 (m, 5H), 7.08 (t, *J* = 8.2 Hz, 2H), 6.98−6.88 (m, 2H), 5.82−5.68 (m, 2H), 5.08 (d, *J* = 10.2 Hz, 1H), 5.02 (d, *J* = 17.0 Hz, 1H), 2.78−2.71 (m, 2H), 2.66−2.54 (m, 2H), 2.25−2.20 (m, 1H), 2.13−2.05 (m, 1H), 1.30 (d, *J* = 7.0 Hz, 3H). LC−MS method 1, t_R = 10.68 min, *m*/*z* = 452. purity = 96%. HRMS calcd for $C_{27}H_{24}F_3NO_2$ + Na 454.1896, found 454.1891.

(*R*)-6-Allyl-3-((*S*)-1-(2′,4′-difluorobiphenyl-4-yl)ethyl)-6-(4-fluorophenyl)-1,3-oxazinan-2-one (*RS*)-23f. ^{1}H NMR ($CDCl_3$) δ 7.33−7.23 (m, 5H), 7.03 (t, *J* = 8.2 Hz, 2H), 6.96−6.86 (m, 4H), 5.77−5.67 (m, 2H), 5.10 (d, *J* = 10.3 Hz, 1H), 5.04 (d, *J* = 17.3 Hz, 1H), 2.99−2.94 (m, 1H), 2.66−2.54 (m, 2H), 2.41−2.34 (m, 1H), 2.30−2.17 (m, 2H), 1.55 (d, *J* = 7.0 Hz, 3H); LC−MS method 2, t_R = 2.13 min, *m*/*z* = 452.

(*S*)-3-((*S*)-1-(2′,4′-Difluoro-[1,1′-biphenyl]-4-yl)ethyl)-6-(4-fluorophenyl)-6-(2-hydroxyethyl)-1,3-oxazinan-2-one (25f). A solution of **23f** (23 g, 43 mmol) in CH_2Cl_2 (250 mL) was cooled to −78 °C, and ozone was bubbled in until the mixture turned blue. $NaBH_4$ (9.8 g, 258 mmol) was added, and the mixture was allowed to warm to room temperature and stirred overnight. Saturated aqueous NH_4Cl was added, and the mixture was extracted with CH_2Cl_2 (3×). The combined organic layer was washed with brine, dried over Na_2SO_4, and concentrated under reduced pressure. The residue was purified by flash chromatography on silica gel, and the more polar isomer was collected. Recrystallization from ethanol afforded **25f** (6.0 g, 25%). ^{1}H NMR (400 MHz, $CDCl_3$) δ 7.24−7.17 (m, 5H), 7.00−6.79 (m, 6H), 5.62 (q, *J* = 7.0 Hz, 1H), 3.74−3.68 (m, 1H), 3.51−3.45 (m, 1H), 2.91−2.88 (m, 1H), 2.30−2.01 (m, 5H), 1.96 (br s, 1H), 1.48 (d, *J* = 7.0 Hz, 3H); ^{19}F NMR (376 MHz, $CDCl_3$) δ −111.61 (m), −114.05 (m), −114.90 (m); ^{13}C NMR (100 MHz, $CDCl_3$) δ 162.28 (dd, *J* = 250.0, 12.3 Hz), 162.17 (d, *J* = 247.7 Hz), 159.66 (dd, *J* = 250.7, 12.3 Hz), 153.03, 138.53, 137.09 (d, *J* = 3.1 Hz), 134.06, 131.24 (dd, *J* = 9.2, 4.6 Hz), 128.70 (d, *J* = 2.3 Hz), 127.09, 126.58 (d, *J* = 8.4 Hz), 124.57 (dd, *J* = 13.8, 3.8 Hz), 115.74 (d, *J* = 21.5 Hz), 111.59 (dd, *J* = 21.5, 3.8 Hz), 104.37 (t, *J* = 26.1 Hz), 82.83, 58.09, 53.18, 44.82, 36.11, 31.75, 15.16; LC−MS method 1, t_R = 8.61 min, *m*/*z* = 456, purity = 100%. Anal. Calcd for $C_{26}H_{24}F_3NO_3$: C, 68.56; H, 5.31; F, 12.51; N, 3.08; O, 10.54. Found: C, 68.53; H, 5.21; N, 3.06.

The less polar diastereomer **24f** exhibited the following spectral characteristics. ^{1}H NMR (400 MHz, $CDCl_3$) δ 7.48−7.30 (m, 7H), 7.13−6.88 (m, 4H), 5.78 (q, *J* = 7.0 Hz, 1H), 3.78−3.74 (m, 1H), 3.57−3.50 (m, 1H), 2.79−2.67 (m, 2H), 2.31−2.11 (m, 4H), 1.81 (br s, 1H), 1.31 (d, *J* = 7.3 Hz, 3H); ^{19}F NMR (376 MHz, $CDCl_3$) δ −111.48 (m), −113.88 (m), −114.67 (m); LC−MS method 2, t_R = 1.86 min, *m*/*z* 456 (MH^+).

(*R*)-3-((*S*)-1-(2′,4′-Difluoro-[1,1′-biphenyl]-4-yl)ethyl)-6-(4-fluorophenyl)-6-(3-hydroxypropyl)-1,3-oxazinan-2-one (25g). To a stirred solution of (*RS*)-**23f** (3.05 g, 6.7 mmol) in THF (40 mL) at 0 °C was added 1 M BH_3 in THF (8.1 mL, 8.1 mmol). The mixture was stirred at room temperature for 2 h, recooled to 0 °C, and treated with water (2 mL), 3 M aqueous NaOH (2 mL, 6 mmol), and 30% aqueous H_2O_2 (2 mL). The mixture was stirred overnight at room temperature, and the pH was adjusted to 6−7 with aqueous HCl. The mixture was extracted with EtOAc (3×). The combined organic layer was washed with saturated aqueous $NaHCO_3$ and brine and dried over Na_2SO_4. Removal of the solvent left a residue which was purified by chromatography on silica gel, followed by preparative HPLC to afford **25g** (700 mg, 22%). ^{1}H NMR ($CDCl_3$) δ 7.34−7.22 (m, 4H), 7.07−6.98 (m, 4H), 6.96−6.85 (m, 3H), 5.69 (q, *J* = 7.02 Hz, 1H),

dx.doi.org/10.1021/jm2005354 |*J. Med. Chem.* 2011, 54, 6050–6062

3.58 (t, J = 6.24 Hz, 1H), 3.10−2.87 (m, 4H), 2.39−2.16 (m, 3H), 2.14−1.89 (m, 2H), 1.56 (d, J = 7.02 Hz, 3H); ^{19}F NMR ($CDCl_3$) −111.60, −114.06, −114.62. LC−MS method 1, t_R = 8.79 min, m/z = 470, purity = 99%. HRMS calcd for $C_{27}H_{26}F_3NO_3$ + Na. 492.1762, found 492.1745.

■ ASSOCIATED CONTENT

Supporting Information. Synthetic procedures and NMR, MS, and HPLC data on new compounds; assay protocols; crystallographic data for **25f**. This material is available free of charge via the Internet at http://pubs.acs.org.

■ AUTHOR INFORMATION

Corresponding Author

*Phone: +1-215-461-2042. Fax: +1-215-461-2006. E-mail: ctice@vitaerx.com.

■ ABBREVIATIONS USED

HPA, hypothalamic−pituitary−adrenal; 11β-HSD1, 11β-hydroxysteroid dehydrogenase type 1; 11β-HSD2, 11β-hydroxysteroid dehydrogenase type 2; DIO, diet-induced obesity; HBA1C, glycosylated hemoglobin

■ REFERENCES

(1) *Diabetes Atlas*, 4th ed.; IDF: Brussels, Belgium, 2009.

(2) Alberti, K. G. M. M.; Eckel, R. H.; Grundy, S. M.; Zimmet, P. Z.; Cleeman, J. I.; Donato, K. A.; Fruchart, J.-C.; James, W. P. T.; Loria, C. M.; Smith, S. C., Jr. Harmonizing the metabolic syndrome: a joint interim statement of the International Diabetes Federation Task Force on Epidemiology and Prevention; National Heart, Lung, and Blood Institute; American Heart Association; World Heart Federation; International Atherosclerosis Society; and International Association for the Study of Obesity. *Circulation* **2009**, *120*, 1640–1645.

(3) Mohler, M. L.; He, Y.; Wu, Z.; Hwang, D. J.; Miller, D. D. Recent and emerging anti-diabetes targets. *Med. Res. Rev.* **2009**, *29*, 125–195.

(4) Tanaka, N.; Nonaka, T.; Nakamura, K. T.; Hara, A. SDR: structure, mechanism of action, and substrate recognition. *Curr. Org. Chem.* **2001**, *5*, 89–111.

(5) Bray, J. E.; Marsden, B. D.; Oppermann, U. The human short-chain dehydrogenase/reductase (SDR) superfamily: a bioinformatics summary. *Chem.-Biol. Interact.* **2009**, *178*, 99–109.

(6) Jacobson, L. Hypothalamic−pituitary−adrenocortical axis regulation. *Endocrinol. Metab. Clin. North Am.* **2005**, *34*, 271–292.

(7) Harno, E.; White, A. Will treating diabetes with 11beta-HSD1 inhibitors affect the HPA axis? *Trends Endocrinol. Metab.* **2010**, *21*, 619–627.

(8) Albiston, A. L.; Obeyesekere, V. R.; Smith, R. E.; Krozowski, Z. S. Cloning and tissue distribution of the human 11beta-hydroxysteroid dehydrogenase type 2 enzyme. *Mol. Cell. Endocrinol.* **1994**, *105*, R11–R17.

(9) Cooper, M. S.; Stewart, P. M. 11beta-Hydroxysteroid dehydrogenase type 1 and its role in the hypothalamus−pituitary−adrenal axis, metabolic syndrome, and inflammation. *J. Clin. Endocrinol. Metab.* **2009**, *94*, 4645–4654.

(10) Wamil, M.; Seckl, J. R. Inhibition of 11beta-hydroxysteroid dehydrogenase type 1 as a promising therapeutic target. *Drug Discovery Today* **2007**, *12*, 504–520.

(11) Fotsch, C.; Wang, M. Blockade of glucocorticoid excess at the tissue level: inhibitors of 11beta-hydroxysteroid dehydrogenase type 1 as a therapy for type 2 diabetes. *J. Med. Chem.* **2008**, *51*, 4851–4857.

(12) Saiah, E. The role of 11beta-hydroxysteroid dehydrogenase in metabolic disease and therapeutic potential of 11beta-HSD1 inhibitors. *Curr. Med. Chem.* **2008**, *15*, 642–649.

(13) Walker, B. R.; Andrew, R. Tissue production of cortisol by 11beta-hydroxysteroid dehydrogenase type 1 and metabolic disease. *Ann. N.Y. Acad. Sci.* **2006**, *1083*, 165–184.

(14) Tomlinson, J. W.; Stewart, P. M. Modulation of glucocorticoid action and the treatment of type-2 diabetes. *Best Pract. Res., Clin. Endocrinol. Metab.* **2007**, *21*, 607–619.

(15) Bertagna, X.; Guignat, L.; Groussin, L.; Bertherat, J. Cushing's disease. *Best Pract. Res., Clin. Endocrinol. Metab.* **2009**, *23*, 607–623.

(16) Masuzaki, H.; Paterson, J.; Shinyama, H.; Morton, N. M.; Mullins, J. J.; Seckl, J. R.; Flier, J. S. A transgenic model of visceral obesity and the metabolic syndrome. *Science (Washington, DC, U. S.)* **2001**, *294*, 2166–2170.

(17) Masuzaki, H.; Yamamoto, H.; Kenyon, C. J.; Elmquist, J. K.; Morton, N. M.; Paterson, J. M.; Shinyama, H.; Sharp, M. G. F.; Fleming, S.; Mullins, J. J.; Seckl, J. R.; Flier, J. S. Transgenic amplification of glucocorticoid action in adipose tissue causes high blood pressure in mice. *J. Clin. Invest.* **2003**, *112*, 83–90.

(18) Kotelevitsev, Y.; Holmes, M. C.; Burchell, A.; Houston, P. M.; Schmoll, D.; Jamieson, P.; Best, R.; Brown, R.; Edwards, C. R. W.; Seckl, J. R.; Mullins, J. J. 11beta-Hydroxysteroid dehydrogenase type 1 knockout mice show attenuated glucocorticoid-inducible responses and resist hyperglycemia on obesity or stress. *Proc. Natl. Acad. Sci. U.S.A.* **1997**, *94*, 14924–14929.

(19) Morton, N. M.; Paterson, J. M.; Masuzaki, H.; Holmes, M. C.; Staels, B.; Fievet, C.; Walker, B. R.; Flier, J. S.; Mullins, J. J.; Seckl, J. R. Novel adipose tissue-mediated resistance to diet-induced visceral obesity in 11beta-hydroxysteroid dehydrogenase type 1-deficient mice. *Diabetes* **2004**, *53*, 931–938.

(20) Morton, N. M.; Holmes, M. C.; Fievet, C.; Staels, B.; Tailleux, A.; Mullins, J. J.; Seckl, J. R. Improved lipid and lipoprotein profile, hepatic insulin sensitivity, and glucose tolerance in 11beta-hydroxysteroid dehydrogenase type 1 null mice. *J. Biol. Chem.* **2001**, *276*, 41293–41300.

(21) Andrews, R. C.; Rooyackers, O.; Walker, B. R. Effects of the 11beta-hydroxysteroid dehydrogenase inhibitor carbenoxolone on insulin sensitivity in men with type 2 diabetes. *J. Clin. Endocrinol. Metab.* **2003**, *88*, 285–291.

(22) Sandeep, T. C.; Andrew, R.; Homer, N. Z. M.; Andrews, R. C.; Smith, K.; Walker, B. R. Increased in vivo regeneration of cortisol in adipose tissue in human obesity and effects of the 11beta-hydroxysteroid dehydrogenase type 1 inhibitor carbenoxolone. *Diabetes* **2005**, *54*, 872–879.

(23) Barf, T.; Vallgårda, J.; Emond, R.; Haeggstroem, C.; Kurz, G.; Nygren, A.; Larwood, V.; Mosialou, E.; Axelsson, K.; Olsson, R.; Engblom, L.; Edling, N.; Roenquist-Nii, Y.; Oehman, B.; Alberts, P.; Abrahmsen, L. Arylsulfonamidothiazoles as a new class of potential antidiabetic drugs. Discovery of potent and selective inhibitors of the 11beta-hydroxysteroid dehydrogenase type 1. *J. Med. Chem.* **2002**, *45*, 3813–3815.

(24) St. Jean, D. J., Jr.; Wang, M.; Fotsch, C. Inhibitors of 11beta-HSD1: a potential treatment for the metabolic syndrome. *Curr. Top. Med. Chem. (Sharjah, United Arab Emirates)* **2008**, *8*, 1508–1523.

(25) Boyle, C. D. Recent advances in the discovery of 11beta-HSD1 inhibitors. *Curr. Opin. Drug Discovery Dev.* **2008**, *11*, 495–511.

(26) Schnackenberg, C. G. 11beta-Hydroxysteroid dehydrogenase type 1 inhibitors for metabolic syndrome. *Curr. Opin. Invest. Drugs (Thomson Sci.)* **2008**, *9*, 295–300.

(27) Hermanowski-Vosatka, A.; Balkovec, J. M.; Cheng, K.; Chen, H. Y.; Hernandez, M.; Koo, G. C.; Le Grand, C. B.; Li, Z.; Metzger, J. M.; Mundt, S. S.; Noonan, H.; Nunes, C. N.; Olson, S. H.; Pikounis, B.; Ren, N.; Robertson, N.; Schaeffer, J. M.; Shah, K.; Springer, M. S.; Strack, A. M.; Strowski, M.; Wu, K.; Wu, T.; Xiao, J.; Zhang, B. B.; Wright, S. D.; Thieringer, R. 11beta-HSD1 inhibition ameliorates metabolic syndrome and prevents progression of atherosclerosis in mice. *J. Exp. Med.* **2005**, *202*, 517–527.

(28) Veniant, M. M.; Hale, C.; Hungate, R. W.; Gahm, K.; Emery, M. G.; Jona, J.; Joseph, S.; Adams, J.; Hague, A.; Moniz, G.; Zhang, J.; Bartberger, M. D.; Li, V.; Syed, R.; Jordan, S.; Komorowski, R.; Chen,

M. M.; Cupples, R.; Kim, K. W.; St. Jean, D. J.; Johansson, L.; Henriksson, M. A.; Williams, M.; Vallgarda, J.; Fotsch, C.; Wang, M. Discovery of a potent, orally active 11.beta-hydroxysteroid dehydrogenase type 1 inhibitor for clinical study: identification of (*S*)-2-((1*S*,2*S*,4*R*)-bicyclo[2.2.1]heptan-2-ylamino)-5-isopropyl-5-methylthiazol-4(5*H*lic>)-one (AMG 221). *J. Med. Chem.* **2010**, *53*, 4481–4487.

(29) Sundbom, M.; Kaiser, C.; Bjoerkstrand, E.; Castro, V. M.; Larsson, C.; Selen, G.; Nyhem, C. S.; James, S. R. Inhibition of 11beta HSD1 with the *S*-phenylethylaminothiazolone BVT116429 increases adiponectin concentrations and improves glucose homeostasis in diabetic KKAy mice. *BMC Pharmacol.* **2008**, *8*, 3.

(30) Hale, C.; Veniant, M.; Wang, Z.; Chen, M.; McCormick, J.; Cupples, R.; Hickman, D.; Min, X.; Sudom, A.; Xu, H.; Matsumoto, G.; Fotsch, C.; St. Jean, D. J., Jr.; Wang, M. Structural characterization and pharmacodynamic effects of an orally active 11beta-hydroxysteroid dehydrogenase type 1 inhibitor. *Chem. Biol. Drug Des.* **2008**, *71*, 36–44.

(31) Wan, Z.-K.; Chenail, E.; Xiang, J.; Li, H.-Q.; Ipek, M.; Bard, J.; Svenson, K.; Mansour, T. S.; Xu, X.; Tian, X.; Suri, V.; Hahm, S.; Xing, Y.; Johnson, C. E.; Li, X.; Qadri, A.; Panza, D.; Perreault, M.; Tobin, J. F.; Saiah, E. Efficacious 11β-hydroxysteroid dehydrogenase type I inhibitors in the diet-induced obesity mouse model. *J. Med. Chem.* **2009**, *52*, 5449–5461.

(32) Whittamore, P. R. O. Discovery of a Potent, Selective and Orally Bioavailable Acidic 11beta-Hydroxysteroid Dehydrogenase Type 1 (11beta-HSD1) Inhibitor. Presented at EFMC-ISMC 2010, Brussels, Belgium, 2010.

(33) Rosenstock, J.; Banarer, S.; Fonseca, V. A.; Inzucchi, S. E.; Sun, W.; Yao, W.; Hollis, G.; Flores, R.; Levy, R.; Williams, W. V.; Seckl, J. R.; Huber, R. The 11-beta-hydroxysteroid dehydrogenase type 1 inhibitor INCB13739 improves hyperglycemia in patients with type 2 diabetes inadequately controlled by metformin monotherapy. *Diabetes Care* **2010**, *33*, 1516–1522.

(34) Feig, P. U.; Shah, S.; Hermanowski-Vosatka, A.; Plotkin, D.; Springer, M. S.; Donahue, S.; Thach, C.; Klein, E. J.; Lai, E.; Kaufman, K. D. Effects of an 11β-hydroxysteroid dehydrogenase type 1 inhibitor, MK-0916, in patients with type 2 diabetes mellitus and metabolic syndrome. *Diabetes, Obes. Metab.* **2011**, *13*, 498–504.

(35) Zhang, J.; Osslund, T. D.; Plant, M. H.; Clogston, C. L.; Nybo, R. E.; Xiong, F.; Delaney, J. M.; Jordan, S. R. Crystal structure of murine 11beta-hydroxysteroid dehydrogenase 1: an important therapeutic target for diabetes. *Biochemistry* **2005**, *44*, 6948–6957.

(36) Patel, J. R.; Shuai, Q.; Dinges, J.; Winn, M.; Pliushchev, M.; Fung, S.; Monzon, K.; Chiou, W.; Wang, J.; Pan, L.; Wagaw, S.; Engstrom, K.; Kerdesky, F. A.; Longenecker, K.; Judge, R.; Qin, W.; Imade, H. M.; Stolarik, D.; Beno, D. W. A.; Brune, M.; Chovan, L. E.; Sham, H. L.; Jacobson, P.; Link, J. T. Discovery of adamantane ethers as inhibitors of 11beta-HSD-1: synthesis and biological evaluation. *Bioorg. Med. Chem. Lett.* **2007**, *17*, 750–755.

(37) Andersson, A.; Jordan, D.; Schneider, G.; Lindqvist, Y. Crystal structure of the ternary complex of 1,3,8-trihydroxynaphthalene reductase from *Magnaporthe grisea* with NADPH and an active-site inhibitor. *Structure (London)* **1996**, *4*, 1161–1170.

(38) "Contour" is a structure-based drug design tool that grows molecules in silico, in the context of a protein binding site, by addition of fragments to a user selected starting template: Singh, S. B. Manuscript in preparation.

(39) Solly, K.; Mundt, S. S.; Zokian, H. J.; Ding, G. J.-F.; Hermanowski-Vosatka, A.; Strulovici, B.; Zheng, W. High-throughput screening of 11beta-hydroxysteroid dehydrogenase type 1 in scintillation proximity assay format. *Assay Drug Dev. Technol.* **2005**, *3*, 377–384.

(40) Nagao, M.; Yahagi, T.; Honda, M.; Seino, Y.; Matsushima, T.; Sugimura, T. Demonstration of mutagenicity of aniline and *o*-toluidine by norharman. *Proc. Jpn. Acad., Ser. B* **1977**, *53*, 34–37.

(41) Hecht, S. S.; El-Bayoumy, K.; Tulley, L.; LaVoie, E. Structure–mutagenicity relationships of N-oxidized derivatives of aniline, *o*-toluidine, 2′-methyl-4-aminobiphenyl, and 3,2′-dimethyl-4-aminobiphenyl. *J. Med. Chem.* **1979**, *22*, 981–987.